 CMES, vol.65, no.1, pp.75-92, 2010

Assessment of Pressure Waves Generated by Explosive Loading

D. Kakogiannis[1], D. Van Hemelrijck[1], J. Wastiels[1], S. Palanivelu[2], W. Van Paepegem[2], J. Vantomme[3], A. Kotzakolios[4] and V. Kostopoulos[4]

Abstract: In the present study the estimation of the blast wave by two types of finite element methods is investigated: Eulerian multi-material modeling and pure Lagrangian. The main goal is to compare and study their ability to predict the clearing effect during blast. Element shape and improvements on the codes are also considered. For the Lagrangian finite element models the load is applied by using an empirical method, deriving from databases, for the time-spatial distribution of the pressure profiles. In the ideal case of the above method the blast load is applied as an equivalent triangular pulse to represent the decay of the incident and reflected pressure. The implementation of this method in LS-DYNA is improved and takes a more realistic approach, assuming an exponential decay of the pressure with time. In the case of the Eulerian models the influence of the shape of elements and its influence on the incident and reflected pressure in three types of simulations, using rectangular, cylindrical and spherical grid of air, were investigated. An analytical method to predict impulse is used to compare with the numerical and experimental results. The Eulerian models provide results closer to the experimental. Specifically, the cylindrical grid of air gives better results in comparison with the other methods.

Keywords: Blast Load, Numerical Simulation, LS-DYNA, ConWep, Finite Element, Clearing Effect.

[1] Department of Mechanics of Materials and Constructions, Brussels, Belgium
[2] Department of Materials Science and Engineering, Gent, Belgium
[3] Civil and Material Engineering Department, Royal Military Academy, Brussels, Belgium
[4] Applied Mechanics Laboratory, Department of Mechanical Engineering and Aeronautics, University of Patras, Patras, Greece

1 Introduction

Experimental and numerical studies have been carried out over the past few years in order to evaluate structures under blast loads and estimate the blast wave parameters. Applications where structures are subjected to blast loads lead to additional design requirements but the optimization of protective structures against blast loads using full-scale experimental tests, is often difficult and expensive. Analytical and numerical methods have been used to analyze the response of structures under explosion and model the blast wave [Ngo, Mendis, Gupta, and Ramsay (2007)]. Attention is turned towards advanced numerical tools like the finite element methods(FEM).

The blast load can be defined by different methods and approaches in finite elements. For the pure Lagrangian approach the blast load is applied on the structure as rectangular or triangular impulse and it is calculated analytically by the response of the experimental setup [Karagiozova, Nurick, and Yuen (2005); Karagiozova, Nurick, and Langdon (2009); Yuen and Nurick (2005); Langdon, Yuen, and Nurick (2005); Balden and Nurick (2005)]. Another way to insert the blast load is by using empirical methods and databases for the time-spatial distribution of the pressure profile such as the computer program ConWep, which is also implemented in LS-DYNA [Kingery and Bulmash (1984)]. In the ideal case of ConWep the structure is considered to be rigid and its surface infinite, as a result the pressure wave applied on the structure is considered as a triangular impulse. The implementation of ConWep in LS-DYNA is improved by introducing a decay coefficient taking into account geometry changes [Randers-Pehrson and Bannister (1997); LSTC (2007)].

One of the methods that has been developed the latest years is the Arbitrary Lagrangian Eulerian(ALE) approach. The ALE multi-material formulation is a method allowing the finite element mesh to move independently from the material flow and each element in the mesh can contain a mixture of two or more different materials [Alia and Souli (2006); Souli, Olovsson, and Do (2002); Souli, Ouahsine, and Lewin (2000)]. The Eulerian multi-material approach is a particular case of ALE where the mesh is fixed and the material flows through it. A coupling algorithm is used to couple the elements of the fluid with the Lagrangian elements of the structure. The Eulerian multi-material formulation provides the most complete description of the blast wave [Børvik, Hanssen, Langseth, and Olovsson (2009)]. Its main disadvantage is the mesh dependency, which is related to the high computational cost.

As it is expected, the different methods do not give the same results and estimations of the blast response of structures. Hydrocodes, in comparison with empirical analytical methods, provide more accurate results especially when structures have

complex geometries, where reflections and shadowing are involved [Luccioni, Ambrosini, and Danesi (2006); Remennikov and Rose (2005); Lu and Wang (2005)]. In some cases the time duration of the blast wave and the peak force do not provide enough information for the blast. If this incomplete information is used in finite elements the results of the simulation do not match with reality. The stiffness of the structure, the area subjected under the blast and the movement of the structure during blast, play important role in the estimation of the blast in combination with the assumptions made for each method [Gantes and Pnevmatikos (2004); Hanssen, Enstock, and Langseth (2004); Zhu, Zhao, Lu, and Gad (2009)].

One of the issues in blast waves, that needs to be taken into account, is the clearing effect or the fast decay of the blast wave, which leads to decrease of the impulse [Smith, Rose, and Saotonglang (1999)]. The present study belongs to that case, where a unidirectionally reinforced pultruded composite tube is axially loaded, in order to study its response under blast load. As a first step triangual pressure profiles, calculated with ConWep, are used to create a Lagrangian finite element model where the composite tube is failing after the application of the load. The experimental result comes in contrast with the simulation and no failure is observed on the tube, which remains intact after the blast. More simulation efforts are invested in order to compare and study the ability of the aforementioned methods to predict the clearing effect, which is considered the main reason for the discrepancy between numerical and experimental results. Specifically, in the Eulerian method the influence of the shape of elements on the coupling is investigated and is compared with the idealized and implemented version of ConWep pressure profiles in LS-DYNA.

2 Experimental Setup

A spherical charge of $30g$ of C4 in a stand off distance of $300mm$ is used to accelerate a cover plate which is in contact with the specimen. The specimen is a pultruded composite tube made of vinyl ester matrix unidirectionally reinforced with glass fibers. The weight of the cover plate is $1.124kg$ and it is constrained to move towards the axial direction of the tube in order to compress it. The specimen is placed on a cylindrical base where a force transducer is measuring the contact force while the blast load is applied on the cover plate. The length of the tube is $100mm$, its outer diameter is $25mm$ and it has wall thickness of $1.5mm$. One edge of the tube was cut in a tulip pattern to create a triggering of 45^o, as shown in Figure 1.

The reflected pressure is measured by a pressure transducer attached on the cover plate and the incident pressure by a blast pencil [Walter (2004)] on the side of the explosive in an angle of 45^o as shown in Figure 2.

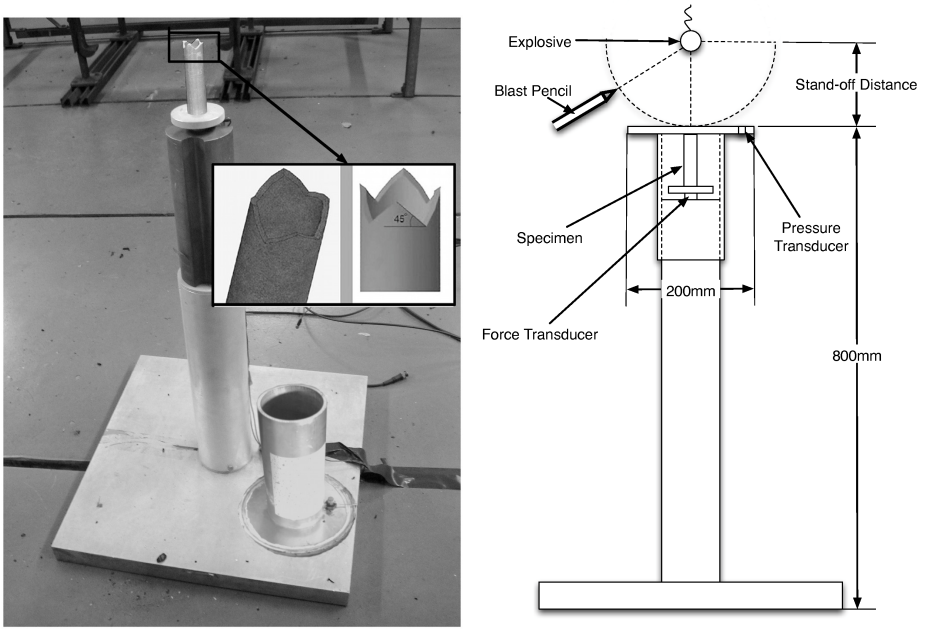

(a) (b)

Figure 1: The experimental setup

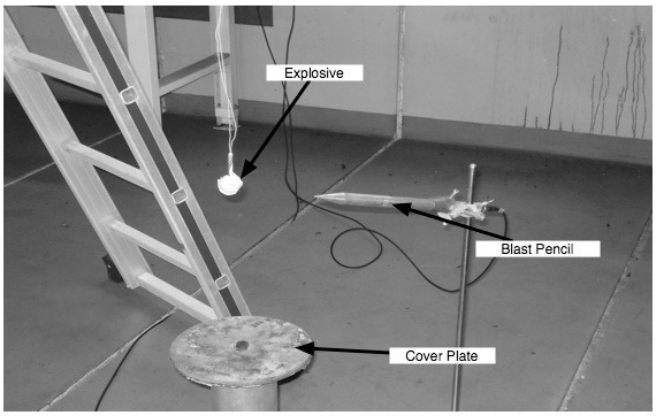

Figure 2: The top side of the experimental setup

The base of the setup, where the tube is placed has vents though which the compressed air can escape during the compression of the tube. The cover plate provides full protection on the sides of tube in order to block the pressure wave that travels around the whole setup after the detonation. The top side of the plate that is subjected to the blast load has a diameter of $200mm$. After the explosive is detonated a spherical pressure wave is created and traveling through air hits the cover plate. The cover plate is in contact with the composite tube that is placed on the instrumented base where the contact force is measured. The full experimental setup is shown in Figure 1. Two experiments are conducted with identical charge and stand off distance that was mentioned before, in both cases there is no failure of the composite pultruded tube.

3 Numerical Modeling

Two types(ConWep and Eulerian multi-material) of simulations have been conducted in order to calculate the pressures applied on the cover plate and the contact force at the base of the tube, during the explosion. Comparison with experimental results is made in order to evaluate the different approaches.

3.1 Model Description

3.1.1 ConWep

The first type of simulations is based on an empirical method that is developed by Kingery and Bulmash [Kingery and Bulmash (1984)] where air blast parameters from spherical air bursts and from hemispherical surface bursts are predicted by equations. These equations are widely accepted as engineering predictions for determining free-field pressures and loads on structures. The Kingery-Bulmash equations have been automated in the computer program ConWep using curve-fitting techniques to represent the data with high-order polynomial equations. Unlike the Kingery-Bulmash equations, where an approximate equivalent triangular pulse is proposed to represent the decay of the incident and reflected pressure, ConWep takes a more realistic approach, assuming an exponential decay of the pressure with time:

$$P(t) = P_{inc}[1 - \frac{t - t_a}{t_+}]exp[-\frac{a(t - t_a)}{t_+}] \tag{1}$$

The objective of this algorithm is to produce an appropriate pressure history given an equivalent TNT explosive weight. The quantities to be determined by the algorithm are:

-P_{inc} : maximum incident pressure,
-P_{ref} : maximum reflected pressure,
-t_a : time of arrival of the shock wave,
-t_+ : positive phase duration,
-a, b : exponential decay factors (wave form numbers) for incident and reflects waves, respectively,
-R : range from charge location to the centroid of loaded surface,
-$cos\theta$: cosine of the incident angle; angle between surface normal and range unit vector.

In the idealized case of ConWep, as the Kingery-Bulmash equations suggest, the impulse is considered triangular because the structure is considered to be rigid and the area of its surface infinite. ConWep is implemented in LS-DYNA by Randers-Pehrson and Bannister and takes into account the decay coefficient which also updates the pressure history based on changes in the geometry [Randers-Pehrson and Bannister (1997); LSTC (2007)]. The parameters that need to be defined by the user are the TNT–equivalent mass of the explosive and the position of the center of the explosion in space, in order the stand off distance to be defined. The disadvantage of this method is that the shorter the stand off distance, the less accurate it is due to the fact that for some parameters there was little or no data near the surface of the charge [Kingery and Bulmash (1984)]. Note that one simulation is performed with ConWep implementation incorporating a decay coefficient and one simulation with the idealized ConWep predictions.

3.1.2 Eulerian muti-material formulation

In the second type of simulations the pressure waves are calculated by multi-material Eulerian formulation, a numerical method based on mathematical equations that describe the basic laws of physics governing the problem. In this method materials flow through a mesh that is completely fixed in space as shown in Fig. 3. An element can contain more than one fluid materials. For the explosion problem, an element may contain one or two different material, air and gas produced from explosive detonation. At each time step, state variables are computed and stored for each material.

A Lagrangian structure can interact with the Eulerian grid through an Eulerian-Lagrangian coupling algorithm [LSTC (2007)]. The fluid-structure interaction in LS-DYNA is modeled with the algorithm *CONSTRAINED_ LAGRANGE_ IN_ SOLID and for the specific study the Donor Cell advection method is used. This method is not free of numerical problems; there is high mesh sensitivity, dissipation and dispersion problems [Souli, Olovsson, and Do (2002); Souli, Ouahsine, and Lewin (2000); Alia and Souli (2006)]. For these reasons three models using the

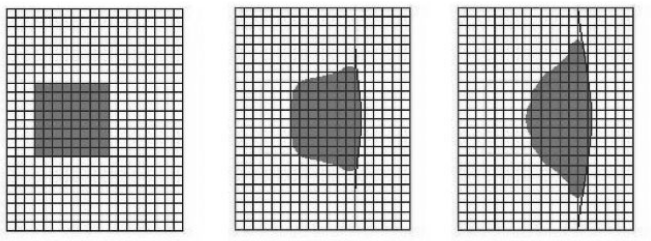

Figure 3: Fluid flowing in Eulerian grid

multi-material Eulerian formulation are created: one with a rectangular grid of air, one with a cylindrical grid of air and one with a spherical grid of air in order to investigate the influence of the shape of elements to the estimation of the pressures and impulses. In both cases a $\frac{1}{4}$ symmetry model is constructed for simulation to reduce computational time. Consequently two planes of symmetry are applied to the model. Non–reflecting boundary conditions are imposed on all the other planes. The smallest size of the elements is 1.7mm near the explosive, the choice is made after making a mesh sensitivity analysis increasing the number of elements until convergence is achieved.

3.2 Geometry

The two types of simulation have common Lagrangian parts where the pressure is applied by the two different methods. The Lagrangian part of the finite element models consists of three parts:
i) the cover plate
ii) the composite pultruded tube
iii) the total base of the setup.
The cover plate and the the base of the setup were modeled with 544 and 2460 solid elements respectively. For the tube a single layer consisting of 300 shell elements is used. For all the contacts between the Lagrangian parts the *AUTOMATIC_SURFACE_TO_SURFACE contact algorithm of LS-DYNA was used with no friction.

In the case of the multi-material FEM the Eulerian parts are:
i)the explosive
ii)the air (rectangular, cylindrical or spherical shape)
The explosive is modeled in both cases as a sphere with 3456 solid elements and the ignition point is placed at the centre of it. In both models the charge is surrounded

with the grid of air and at the boundary between them the nodes match one-to-one. The dimensionality of the rectangular grid of air is 1080mm x 600mm in order to include the whole setup with the Langragian elements, 228152 solid elements are used. The cylindrical grid has 300mm radius, 1080mm height and 127680 solid elements are used for the grid of air. The spherical grid has a radius of 1082mm and 43200 elements are used to model it.

3.3 Material Models

The pultruded tube is modeled as an orthotropic material with damage. The Chang and Chang failure criterion is used to calculate, if there is, damage initiation and propagation. The properties of the pultruded tube used in the present analysis are taken by [Sims and Broughton (2000)]. The properties used for the pultruded tube are shown on Table 1.

Table 1: Pultruded tube properties

Elastic Properties				Strength Properties			
$E_{xxT}(GPa)$	31.2	$E_{xxC}(GPa)$	31.2	$\sigma_{xxT}(MPa)$	483	$\sigma_{xxC}(MPa)$	409
$E_{yyT}(GPa)$	9.36	$E_{yyC}(GPa)$	9.36	$\sigma_{yyT}(MPa)$	34.9	$\sigma_{yyC}(MPa)$	92.2
v_{xy}	0.29						
v_{yx}	0.1						
$G_{xy}(GPa)$	7.33			$\tau_{xy}(MPa)$	73.3		

Air is modeled using a hydrodynamic material model which requires an equation of state, density, pressure cut-off and viscosity coefficient to be defined. In the present analysis the pressure cut-off and viscosity are set to zero due to the fact that pressure cannot be negative and viscosity forces are negligible [Alia and Souli (2006)]. The equation of state that is used for air is the polynomial equation:

$$p = C_0 + C_1\mu + C_2\mu^2 + C_3\mu^3 + E(C_4 + C_5\mu + C_6\mu^2) \tag{2}$$

where $\mu = \frac{\rho}{\rho_o}$, ρ and ρ_o are the current and the initial densities of air and E is the specific internal energy. For ideal gas Eq.2 takes the form:

$$p = EC_5\mu = (\gamma - 1)\frac{\rho}{\rho_o} \tag{3}$$

where γ is the polytropic ratio of specific heats and for the air is equal to 1.4. At time $t = 0$ Eq.3 gives an initial pressure $p_o = 100kPa$ for $\gamma = 1.4$ and $E_o = 250kPa$. For the explosive detonation, the Jones–Wilkins–Lee (JWL) equation of state [Alia

and Souli (2006); Souli, Olovsson, and Do (2002)]. is adopted:

$$p_{JWL} = A(1 - \frac{\omega}{R_1 V})exp(-R_1 V) + B(1 - \frac{\omega}{R_2 V})exp(-R_2 V) + \frac{\omega}{V}E \tag{4}$$

where p is the pressure, A, B, R_1, R_2 and ω are constants, V is the specific volume and E is the internal energy per unit volume. The properties of the parameters of air and C4 are presented in Table 2 were V_d is the detonation velocity.

Table 2: Parameters of air and C4

Air Properties		C4 Properties					
γ	1.4	$A(GPa)$	598.1	$E(GPa)$	8.7	ω	0.32
$E_o(GPa)$	250×10^{-6}	$B(GPa)$	13.7	$\rho(g/cm^3)$	1.601		
$\rho_o(g/cm^3)$	1.293×10^{-3}	R_1	4.5	$V_d(cm/\mu sec)$	0.804		
		R_2	1.5	$p_{CJ}(GPa)$	28.1		

The cover plate and the base of the setup are considered to be elastic and typical aluminum properties were used.

4 Analytical determination of Impulse

Incident pressure and impulse are estimated analytically for the purpose to compare with the experimental and numerical results. The peak overpressure P_s and time duration of the wave t_s can be calculated by Eq. 6 and 7 in function of the mass of the charge W and the scaled distance Z as proposed by Kinney and Graham [Yuen, Nurick, Verster, Jacob, Vara, Balden, Bwalya, Govender, and Pittermann (2008)]. The following equations are based on the assumption that the charge is spherical. The scaled distance is calculated by:

$$Z = \frac{R}{W^{\frac{1}{3}}} \tag{5}$$

where R is the stand off distance and W is the equivalent mass of the charge in TNT. The overpressure is calculated by:

$$\frac{P_s}{P_o} = \frac{808(1 + (Z/4.5)^2)}{\sqrt{1 + (Z/0.048)^2}\sqrt{1 + (Z/0.32)^2}\sqrt{1 + (Z/1.35)^2}} \tag{6}$$

where P_o is the atmospheric pressure.

$$\frac{t_s}{W^{1/3}} = \frac{980[1+(Z/0.54)^{10}]}{[1+(Z/0.02)^3][1+(Z/0.74)^6]\sqrt{1+(Z/6.9)^2}} \tag{7}$$

The explosive mass of C4 is converted into TNT equivalent. For the C4 the TNT equivalent conversion factor is 1.2 [Yandzio and Gough (1999)]. Neglecting the negative phase of the pressure-time diagram and assuming a triangular pulse, the applied impulse I can be calculated by:

$$I = \frac{1}{2} A P_s t_s \tag{8}$$

where A is the area subjected under the blast load.

5 Results and Discussion

The reflected pressure, the incident pressure and the contact force were recorded in order to analyze the response of the structure and evaluate the numerical models. In four of the numerical simulations, as in the experiment, under the specific blast load, no failure is observed on the composite pultruded tube. Failure on the tube was observed only in the case of idealized ConWep. The average crushing force of the tube was acquired by conducting quasistatic axial compression on the pultruded tube with a speed of 200mm/min. The force versus displacement plot is shown in Figure 4.

The numerical contact force between the tube and the base was compared with the force transducer output as shown in Figure 5.

The peak forces, for the three simulations, show good correlation with the experimental values but still they are not higher than the force required to initiate failure. In the case of the idealized ConWep calculation, the contact force is much higher and damage is observed. The discontinuities in the force diagram are attributed to the vibration of the total setup during crushing. The contact force becomes zero at the time instants when the tube loses contact with the base.

In Eulerian grids the explosive is burned in 0.00205 *msec* as it is expected which can easily be validated taking into account the detonation velocity. In both grids the wave travels and hits the structure at the same time, creating the reflected pressure wave. The flow of compressed air reaches the edges of the plate where it goes underneath and finally hits the bottom of the setup where it is reflected back. Small differences are noticed in the plot contours of the wave due to the change of shape of the elements.

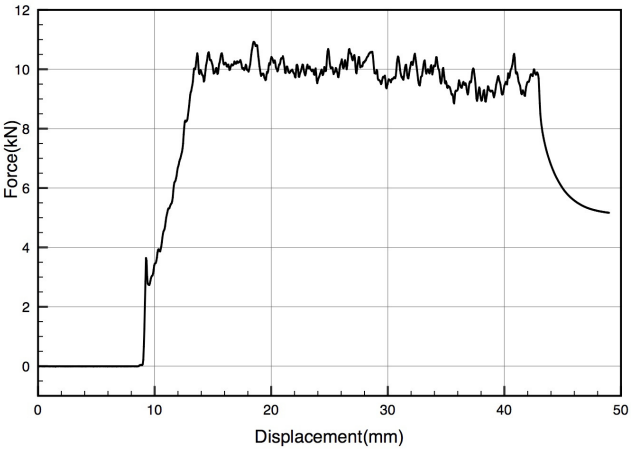

Figure 4: The resultant Force vs Displacement plot from the quasistatic compression

However, in the case of the cylindrical grid the wave propagation is more uniform in comparison with the rectangular grid as it can be seen from Figures 7 and 6. The spherical grid gives even more uniform flow of the pressure wave due to the reason that the wave is spherical and the boundaries of the volume are far form the Langragian elements.

In Table 3 are summarized the results for the incident and reflected pressures and impulses. The incident and reflected pressure are plotted versus time in Figures 9, 10.

Table 3: Comparison between impulses and pressures

	Average Experimental	Analytical	Numerical				
			ConWep		Eulerian		
	–	–	Idealized	With Decay	Rectangular	Cylindrical	Spherical
Incident Impulse(Ns)	1.192	2.75	10.508	2.027	1.486	1.470	1.623
Incident Peak Pressure(GPa)	0.000695	0.00123	0.00121	0.00109	0.000730	0.000742	0.000761
Reflected Impulse(Ns)	10.304	–	61.292	6.041	8.613	8.443	8.603
Reflected Peak Pressure(GPa)	0.00649	–	0.00699	0.00496	0.00355	0.00513	0.00511

In the case of the incident pressure both ConWep approaches overestimate the peak pressure in comparison with Eulerian approach which gives closer results to the experimental. The duration of the pressure wave is accurately calculated by ConWep

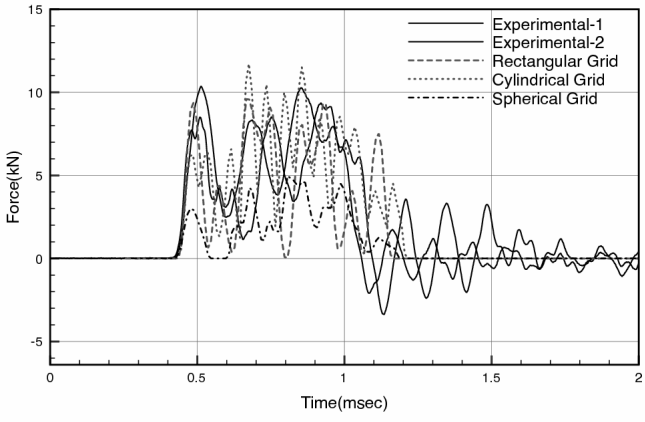

(a) Eulerian grid simulations

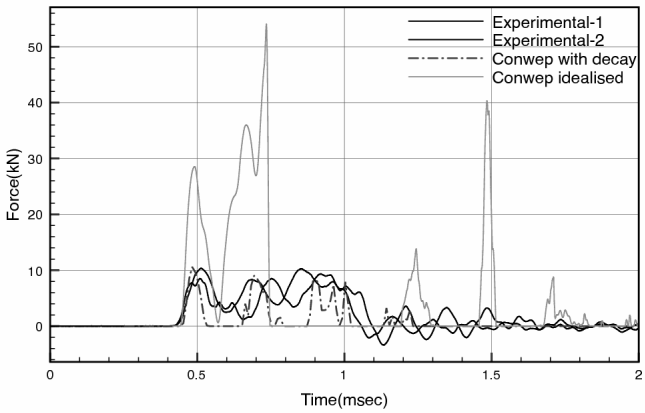

(b) Conwep simulations

Figure 5: Force vs Time

with the decay coefficient, while it is underestimated by the two Eulerian models, it is highly overestimated in the case of idealized ConWep model. The analytical solution predicts the time duration of the pressure wave $(ts = 0.141msec)$ but the value of the peak pressure is closer to the idealized ConWep value.

The reflected pressure plots concluded by Eulerian simulations as well as ConWep with decay coefficient converge better to the experimental results in terms of duration. Idealized ConWep gives much longer duration in comparison with the experimental. The reflected peak pressure is underestimated by all approaches except

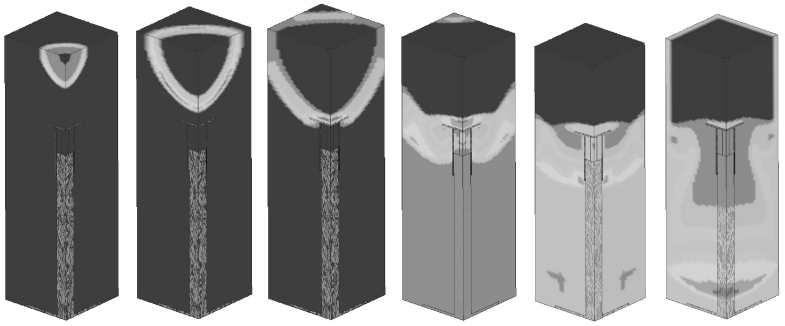

(a) 0.033msec (b) 0.094msec (c) 0.188msec (d) 0.366msec (e) 0.501msec (f) 1.409msec

Figure 6: The contour of pressure for the rectangular grid

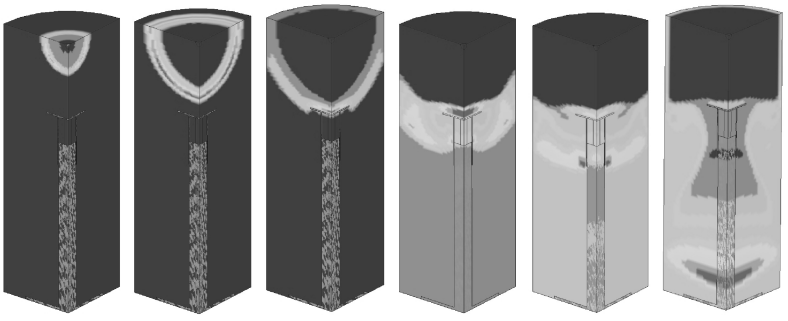

(a) 0.033msec (b) 0.094msec (c) 0.188msec (d) 0.366msec (e) 0.501msec (f) 1.409msec

Figure 7: The contour of pressure for the cylindrical grid

idealized ConWep that gives very good prediction for the peak. Specifically, ConWep with decay and Eulerian approach with cylindrical and spherical grid provide peak pressure results which are closer but lower to the experimental value.

The impulses can be calculated from the pressure curves through integration, the results are shown in Table 3. In terms of incident impulse all methods overestimate it and the Eulerian grids give closer values to the experimental ones. The incident impulse calculated analytically is closer to the value estimated by ConWep with decay. In the case of reflected impulse all methods underestimate it, except idealized ConWep which gives 6 times higher impulse than the experimental.

The fact that there is no clearing effect taken into account is the main reason that idealized ConWep overestimates the values of impulse and pressure. In that case

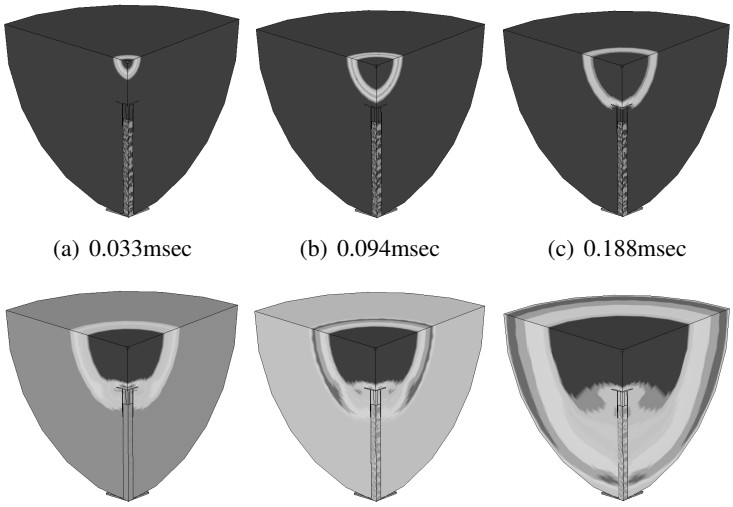

(a) 0.033msec (b) 0.094msec (c) 0.188msec

(d) 0.366msec (e) 0.501msec (f) 1.409msec

Figure 8: The contour of pressure for the spherical grid

the structure is considered to be rigid and its surface, subjected to the blast wave, infinite. The main characteristic of the clearing effect is the loss of impulse which depends on the geometry of the surface of the structure and defines also the form of the pressure curves [Smith, Rose, and Saotonglang (1999); Bangash and Bangash (2006)]. In the experiment, the surface is finite and part of the compressed air flows on the edges which leads to faster decay of the pressure. The difference in peak pressure of ConWep with the decay coefficient is due to the fact that the implementation in LS-DYNA takes into account the changes in the geometry of the structure that is subjected to the blast. As a result, during blast, stiffness and vibration of the cover plate have effect on the reflected pressure curve. The differences in the peak pressures in the case of the Eulerian grids is due to the element shape. The wave that is generated is spherical and the grid in both cases does not follow the pattern of a sphere. The reflected pressure from the Eulerian method is calculated through the coupling between the grid of air and the Lagrangian structure. In the present study the surface of interest of the structure is cylindrical. By using similar pattern in the grid of air better convergence is noticed in the reflected pressure. In general shadowing and multiple reflections are taken into account in the case of the Eulerian multi-material modeling.

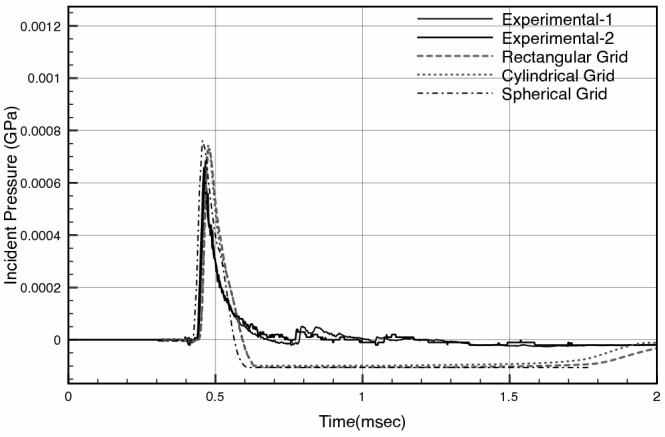

(a) Incident pressure for Eulerian grids

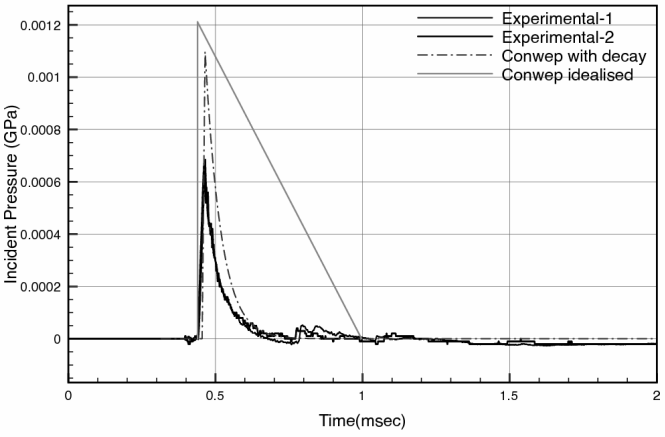

(b) Incident pressure for Conwep models

Figure 9: The plots of incident pressure versus time

6 Conclusions

Two finite element methods are evaluated and compared with experimental results. As it shown from the finite elements models, reflected impulse is a primary damage mechanism since failure of the tube is observed only in the case of idealized ConWep. Taking into account the decay coefficient and geometry changes, ConWep is approaching the experimental results and its main advantage is low computing cost in comparison with the Eulerian method. In total, the combination of both ver-

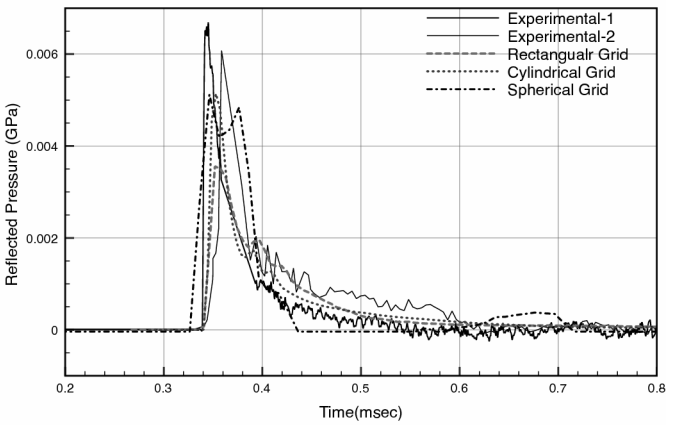

(a) Reflected pressure for Eulerian grids

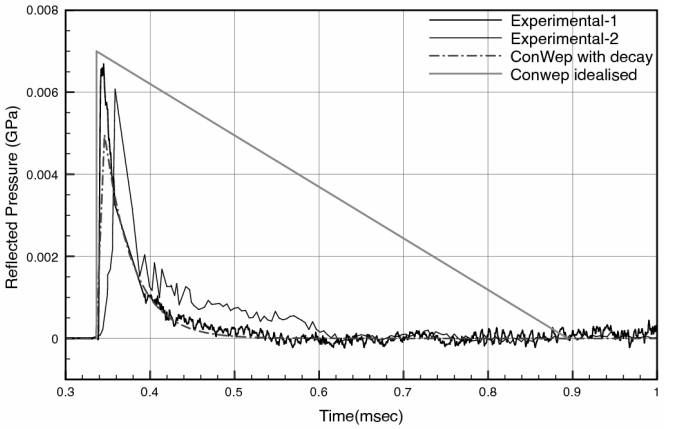

(b) Reflected pressure for Conwep models

Figure 10: The plots of reflected pressure versus time

sions of ConWep can be considered as a conservative design tool. In the Eulerian multi-material method a lot of factors play important role in the estimation of the blast wave. The present study was focused on the influence of the shape of the Eulerian elements in the coupling. More specifically, in the case where the mesh of air follows the same pattern of the mesh structure, better coupling is achieved. With Eulerian methods the pressure wave and its reflections after detonation are also visible and that is an advantage in cases where shadowing creates additional, unexpected, loading on the structure. In the case of the reflected pressure differ-

ences on the peak are noticed. This is due to the fact that the air molecules at the front of the blast wave are stopped abruptly by the presence of the surface which yields. As a result, the stiffness of the structure has influence on the calculation of the peak reflected pressure. In the case of the Eulerian models it is clear that the shape of the elements leads to better coupling and consequently better prediction of the reflected pressure. In cases where the structure has complex geometry, or there is a finite area subjected under blast loads and the energy transfer needs to be studied, ConWep implementation and Eulerian multi material modeling are efficient design tools. The major difference is the calculation time and the experience required in the case of the Eulerian multi-material modeling where a lot of factors such as element size and geometry, advection method and coupling can have effect on the results. On the other hand, in cases where is necessary to have full view of the propagation and reflections of the blast wave, the only method, from the investigated, that can calculate it is the Eulerian.

Acknowledgement: The authors gratefully acknowledge the financial support of the Fund for Scientific Research –Flanders (F.W.O) and thank Dr. Leonard E. Schwer for sharing his expertise in the area of simulation of explosions.

References

Alia, A.; Souli, M. (2006): High explosive simulation using multi-material formulations. *Applied Thermal Engineering*, vol. 26, pp. 1032–1042.

Balden, V.; Nurick, G. N. (2005): Numerical simulation of the post-failure motion of steel plates subjected to blast loading. *International Journal of Impact Engineering*, vol. 32, pp. 14–34.

Bangash, M. Y. H.; Bangash, T. (2006): *Blast and Explosive Loadings on Buildings*. Springer Berlin Heidelberg.

Børvik, T.; Hanssen, A.; Langseth, M.; Olovsson, L. (2009): Response of structures to planar blast loads–A finite element engineering approach. *Computers and Structures*, vol. 87, pp. 507–520.

Gantes, C. J.; Pnevmatikos, N. G. (2004): Elastic–plastic response spectra for exponential blast loading. *International Journal of Impact Engineering*, vol. 30, pp. 323–343.

Hanssen, A. G.; Enstock, L.; Langseth, M. (2004): Close-range blast loading of aluminum foam panels. *International Journal of Impact Engineering*, vol. 27, pp. 593–618.

Karagiozova, D.; Nurick, G. N.; Langdon, G. S. (2009): Behaviour of sandwich panels subject to intense air blasts–Part 2: Numerical simulation. *Composite Structures*, vol. 91, pp. 442–450.

Karagiozova, D.; Nurick, G. N.; Yuen, S. C. K. (2005): Energy absorption of aluminium alloy circular and square tubes under an axial explosive load. *Thin-Walled Structures*, vol. 43, pp. 956–982.

Kingery, C. N.; Bulmash, G. (1984): Air-Blast Parameters from TNT Spherical Airburst and Hemispherical Surface Burst. ABRL-TR-0255. *U. S. Army Ballistic Research laboratory*.

Langdon, G. S.; Yuen, S. C. K.; Nurick, G. N. (2005): Experimental and numerical studies on the response of quadrangular stiffened plates. Part II: localized blast loading. *International Journal of Impact Engineering*, vol. 31, pp. 85–111.

LSTC (2007): *LS-DYNA Keyword User's Manual, Version 971*. Livemore Software Technology Corporation.

Lu, Y.; Wang, Z. (2005): Characterization of structural effects from above-ground explosion using coupled numerical simulation. *Computers and Structures*, vol. 84, pp. 1729–1742.

Luccioni, B.; Ambrosini, D.; Danesi, R. (2006): Blast Load assessment using hydrocodes. *Engineering Structures*, vol. 28, pp. 1736–1744.

Ngo, T.; Mendis, P.; Gupta, A.; Ramsay, J. (2007): Blast Loading and Blast Effects on Structures-An Overview. *EJSE Special Issue: Loading on Structures*, pp. 76–91.

Randers-Pehrson, G.; Bannister, K. (1997): AirBlast Loading Model for DYNA-2D and DYNA-3D. ARL-TR-1310. *Army Research Laboratory*.

Remennikov, A. M.; Rose, T. A. (2005): Modelling blast loads on buildings in complex city geometries. *Computers and Structures*, vol. 83, pp. 2197–2205.

Sims, G. D.; Broughton, W. R. (2000): *Comprehensive Composite Materials*. Elsevier Science.

Smith, P. D.; Rose, T. A.; Saotonglang, E. (1999): Clearing of blast waves from building facades. *Proceedings of the Institution of Civil Engineers*, vol. 134, pp. 193–199.

Souli, M.; Olovsson, L.; Do, I. (2002): ALE and Fluid-Structure Interaction Capabilities in LS-DYNA. *Proceedings of 7th International LS-DYNA Users Conference*.

Souli, M.; Ouahsine, A.; Lewin, L. (2000): ALE formulation for fluid–structure interaction problems. *Computer methods in applied mechanics and engineering*, vol. 190, pp. 659–675.

Walter, P. (2004): Air-blast and the science of dynamic pressure measurements. *Sound and Vibration*, vol. 30, pp. 10–16.

Yandzio, E.; Gough, M. (1999): *Protection of Buildings Against Explosion*. THe Steel Construction Institute.

Yuen, S. C. K.; Nurick, G.; Verster, W.; Jacob, N.; Vara, A.; Balden, V.; Bwalya, D.; Govender, R.; Pittermann, M. (2008): Deformation of mild steel plates subjected to large-scale explosions. *International Journal of Impact Engineering*, vol. 35, pp. 684–703.

Yuen, S. C. K.; Nurick, G. N. (2005): Experimental and numerical studies on the response of quadrangular stiffened plates. Part I: subjected to uniform blast load. *International Journal of Impact Engineering*, vol. 31, pp. 55–83.

Zhu, F.; Zhao, L.; Lu, G.; Gad, E. (2009): A numerical simulation of the blast impact of square metallic sandwich panels. *International Journal of Impact Engineering*, vol. 36, pp. 687–699.